Ultrafast Demagnetization? in Nickel Thin Films

PH5101: MS Project (Autumn)

Abhay Saxena

Mentor: Prof. Kamaraju Natrajan

UFTHz Group
Department of Physical Sciences
IISER Kolkata

December 9, 2025

Overview

Section 1

Setup

Sample

- **Structure:** Cr (∼2nm)-Ni (∼10nm)-Cr (2nm) on Sapphire Substrate.
- **Method:** Electron Beam Evaporation.
- Top layer Chromium likely Cr_2O_3; acts as a passivating layer.
- Bottom Cr acts as a seeding layer.
- Sample transmits ∼32% and reflects ∼36% of a 50μW laser (800nm).

Acknowledgement

I express my sincere gratitude to Prof. Partha Mitra and Mr. Harekrishna Bhunia from the Spintronics Lab for their generosity in providing the necessary samples.

Setup (Schematic)

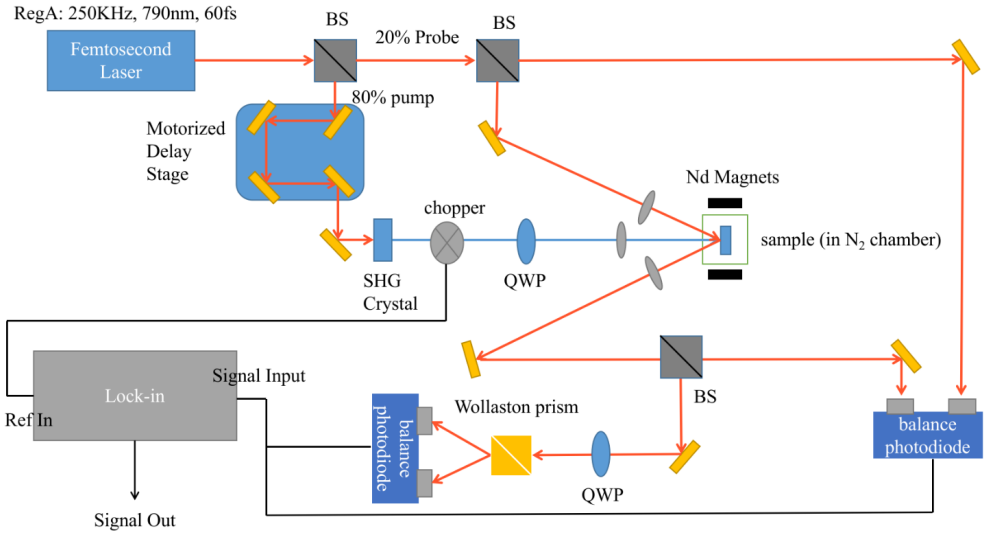

Why Nickel? Electronic Structure and Magnetic Anisotropy

Electronic Configuration & Excitation:

- **Band Structure:** Ni is a prototypical itinerant 3d ferromagnet ($[Ar]3d^8 4s^2$). The magnetic moment ($\sim 0.6\mu_B$) arises from holes in the minority 3d band near the Fermi level ($E_F \approx 5.1eV$). This Excitation needs $\sim 0.1 - 0.8eV$.
- **The Pump Action:** The 400nm (3.1 eV) pump pulse promotes electrons from occupied d-states below E_F to unoccupied sp-states above E_F. This modifies the exchange splitting (ΔE_{ex}) and spin population.

Anisotropy & Domains:

- **Thin Film Anisotropy:** In thin films ($\sim$10-20nm), shape anisotropy ($2\pi M_s^2$) typically forces magnetization in-plane. However, surface anisotropy or strain (from Sapphire substrate) can induce perpendicular magnetic anisotropy (PMA).
- **Single Domain State:** We observe single magnetic domains to minimize exchange energy costs associated with domain walls, dictated by the competition between magnetostatic energy and magnetocrystalline anisotropy (K_u).

Reflectivity Data

$\Delta R/R$ via 800 nm (1.55 eV) probe monitors the Thermomodulation of the dielectric function (Drude-Lorentz contribution).

Demagnetization Origin

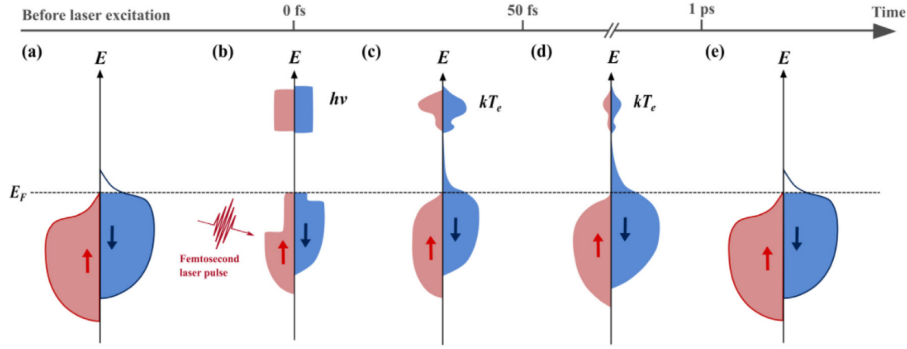

Fig. 9. Schematic representation of the ultrafast demagnetization process in ferromagnets. (a) The density of states in a ferromagnet before laser excitation. (b) Laser excitation leads to unequal excitation of spin-up and spin-down electrons due to the asymmetric distribution of occupied and unoccupied state densities. (c) The electronic system rapidly thermalizes, restoring the Fermi-Dirac distribution, where demagnetization begins as indicated by changes in spin populations. This spin–flip events lead to a decrease in magnetization within 20 fs [251]. (d) The spin–flip scattering of electrons with other quasiparticles, as well as the generation of spin currents, further reduces the magnetization. (e) After 1 ps, the magnetization relaxes, and the DOS of system nearly returns to its initial state.

Section 2

Fluence Dependent Pump Probe

Reflectivity with Pump Fluence

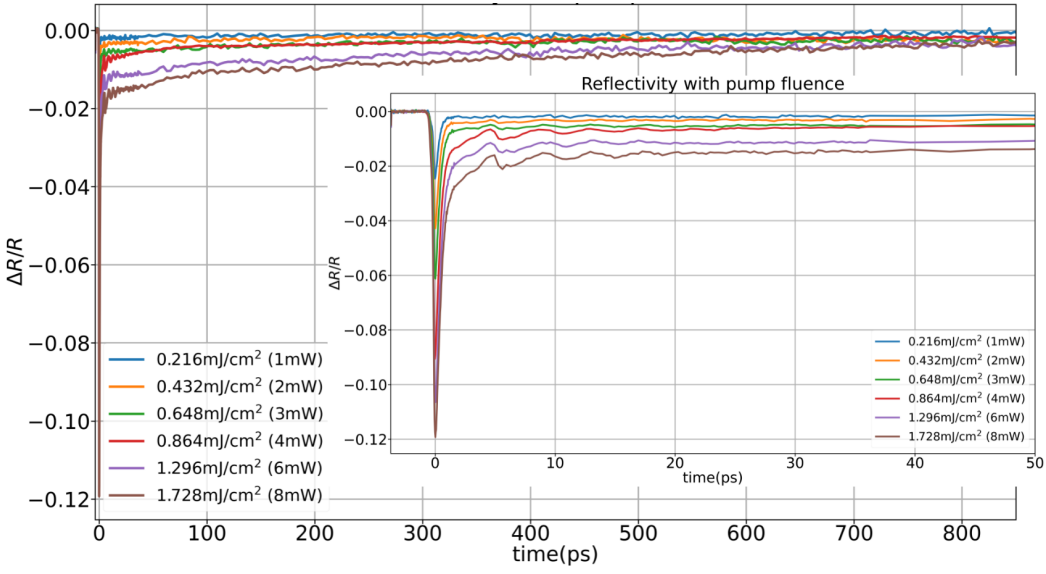

Normalized Reflectivity with Pump Fluence

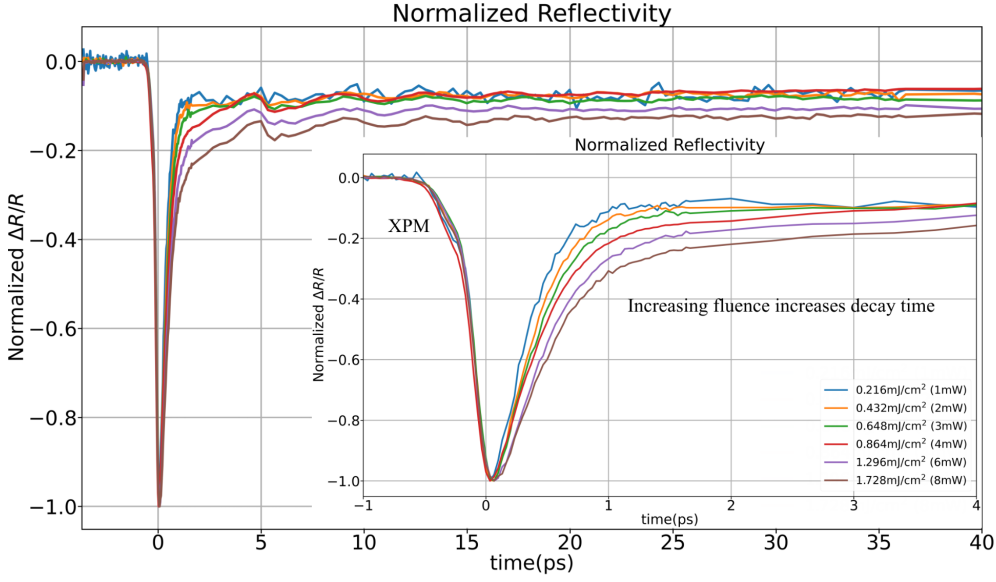

Heatmap Visualization

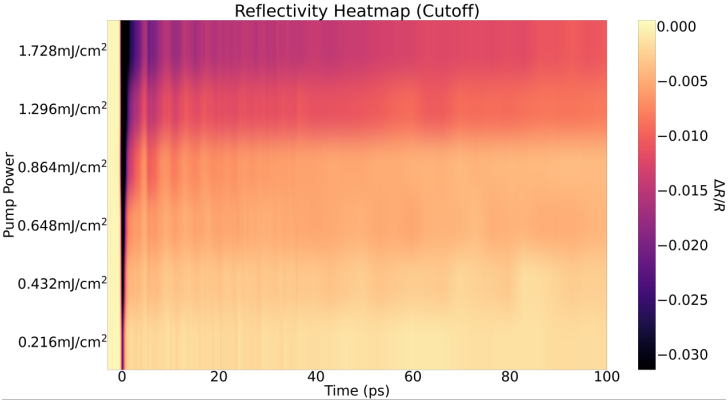

Figure: Unnormalized Case

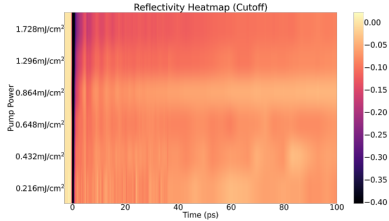

Figure: Normalized Case

Fitting the data

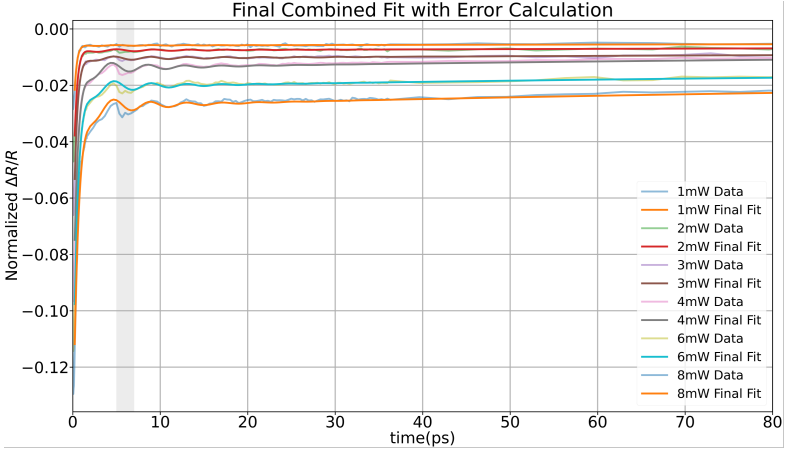

$$y(x) = \underbrace{A_1 e^{-x/\tau_1} + A_2 e^{-x/\tau_2} + A_{3l}\cos(2\pi f_l x + \phi_l) + C_0}_{\text{Background}} + \underbrace{A_{\text{osc}} e^{-x/\tau_{\text{osc}}} \cos\left(2\pi\left(f_0 x + \frac{1}{2}\beta x^2\right) + \phi_{\text{osc}}\right)}_{\text{Acoustic Phonon}} \quad (1)$$

Fitting the data

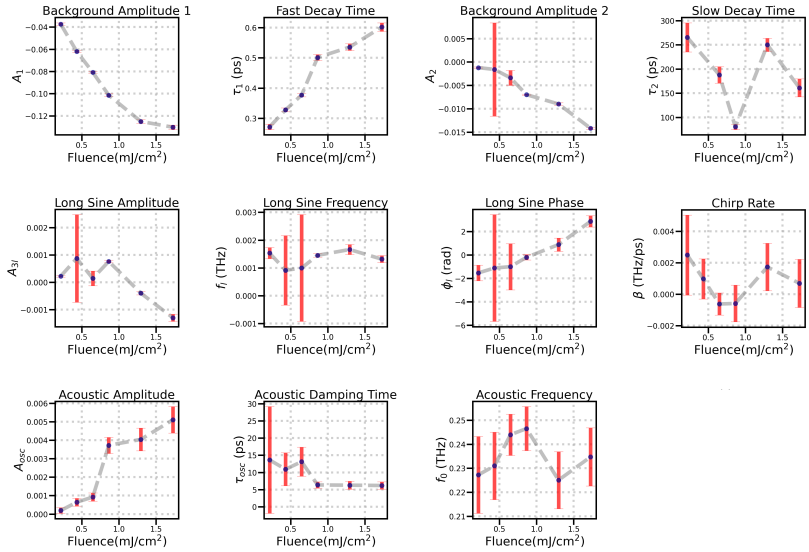

Alternate fitting

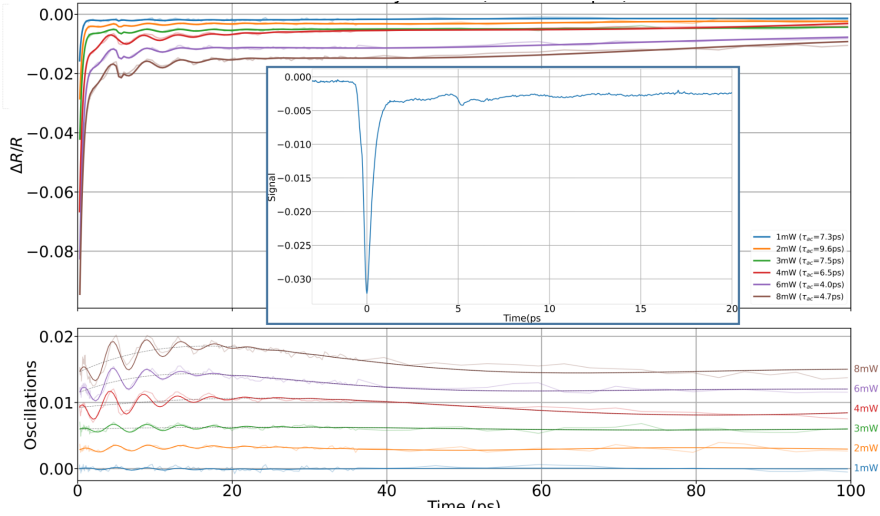

$$\text{reflection} = A_{\text{ref}} \cdot e^{-\frac{(x-t_{\text{ref}})^2}{2w_{\text{ref}}^2}} \qquad \text{at } 5.25\text{ps} \tag{2}$$

Understanding the Probe: Drude-Lorentz & State Filling

What are we actually measuring?
The transient reflectivity $\Delta R/R$ is not a direct "magnetometer". It probes the dielectric function $\epsilon(\omega, T_e, T_l)$. We must decouple electronic heating from lattice dynamics.

Drude-Lorentz Connection

The signal separates into electronic (T_e) and lattice (T_l) contributions:

$$\frac{\Delta R}{R} = \frac{1}{R}\left(\underbrace{\frac{\partial R}{\partial T_e}\Delta T_e}_{\text{Fast Electronic Spike}} + \underbrace{\frac{\partial R}{\partial T_l}\Delta T_l}_{\text{Slow Lattice Heating}} \right) \tag{3}$$

Artifacts vs. Physics:

- **State-Filling (Bleaching):** At $t \approx 0$, the pump depletes occupied d-states and fills sp-states. This blocks probe absorption (Pauli blocking), creating a sharp non-magnetic spike.
- **XPM:** Cross-Phase Modulation may appear as a coherent artifact at $t = 0$ due to pump-probe overlap in the substrate.

Acoustic Phonons: Impedance & Decay

Origin of the ∼4 ps Oscillation

Rapid lattice heating creates thermal stress (σ_{th}), launching a coherent strain pulse (breathing mode) that bounces inside the film.

1. Pulse Period (T_{ac}):

For $d = 10$ nm Ni and sound velocity $v_s \approx 5.6$ nm/ps:

$$T_{ac} = \frac{2d}{v_s} \approx \frac{20 \text{ nm}}{5.6} \approx 3.6 \text{ ps} \qquad (4)$$

(Matches observed ∼4 ps data).

2. Why does it decay so fast?

We calculate the Acoustic Impedance $Z = \rho v$:

- $Z_{\text{Ni}} \approx 50$ MRayl
- $Z_{\text{Sapphire}} \approx 44$ MRayl

Interface Reflectivity Calculation

The intensity reflection coefficient R at the back interface is:

$$R = \left(\frac{Z_{\text{sub}} - Z_{\text{Ni}}}{Z_{\text{sub}} + Z_{\text{Ni}}} \right)^2 \approx \left(\frac{44 - 50}{44 + 50} \right)^2 \approx 0.004 \quad (0.4\%) \qquad (5)$$

Crucial Finding: Only 0.4% of the energy is reflected; 99.6% transmits into the substrate. This massive leakage explains the rapid damping ($\tau \approx 6$ ps) of the acoustic mode.

Section 3

Two Temperature Model and M3TM

Thermodynamics: Two-Temperature Model (2TM) & Spin Temp

We model the thermal evolution of the electron (T_e) and lattice (T_l) baths using the 2TM, and **predict** the effective spin temperature (T_s) from the resulting magnetization dynamics.

1. Laser Source Term $P(t)$

Absorbed power density for a Gaussian pulse:

$$P(t) = \underbrace{\frac{F_{abs}}{d_{film}}}_{\text{Energy Density}} \cdot \frac{1}{\sigma\sqrt{2\pi}} e^{-\frac{t^2}{2\sigma^2}} \tag{6}$$

2. Coupled Heat Equations (2TM)

$$C_e(T_e)\frac{dT_e}{dt} = P(t) - G_{el}(T_e - T_l) \tag{7}$$

$$C_l\frac{dT_l}{dt} = G_{el}(T_e - T_l) \tag{8}$$

Heat Capacities:

- Electrons: $C_e(T_e) = \gamma_e T_e$ (Linear dependence critical for high T_e).
- Lattice: C_l is assumed constant (Debye limit).

2 Temperature Model Fitting to Fluence dependent Result

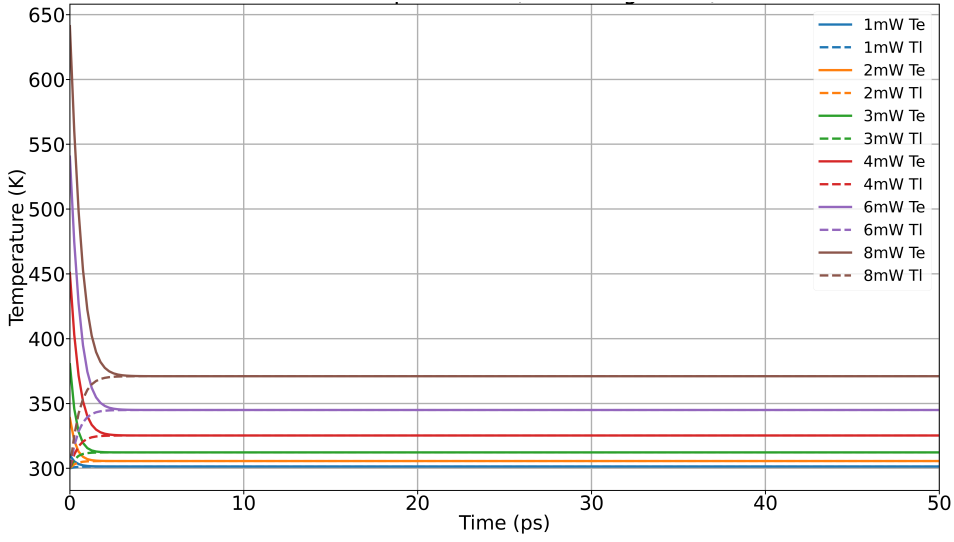

2 Temperature Model Fitting to Fluence dependent Result

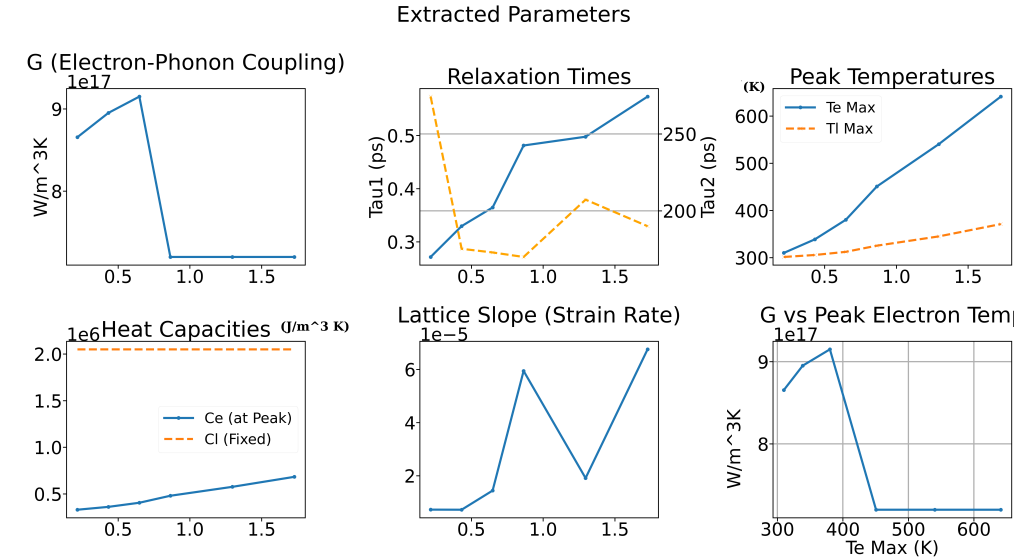

M3TM Prediction of T_s

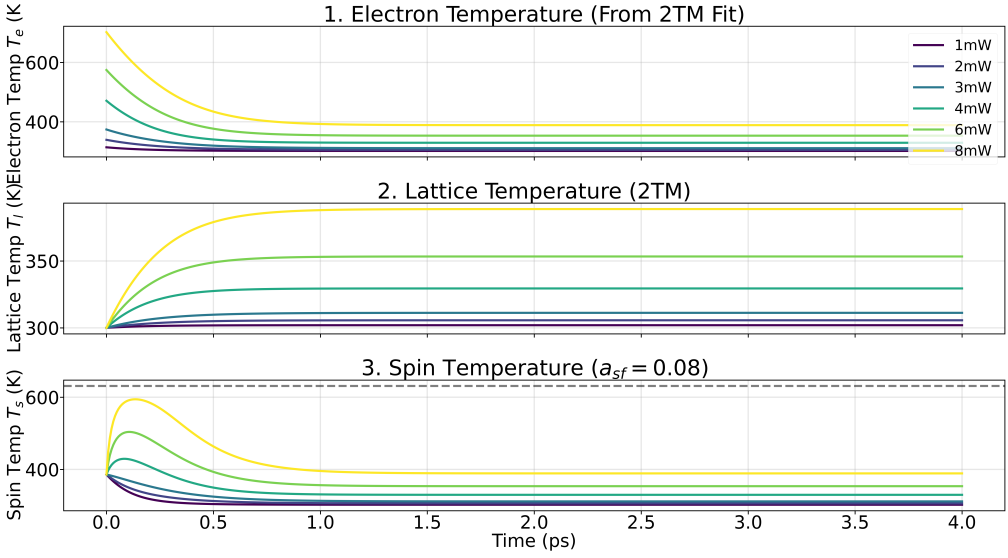

Section 4

Anisotropic Pump Probe

Recovery Dynamics: LLG, Precession & Artifacts

Macroscopic Recovery ($t > 100$ ps)
The slow sine wave ($\sim$1000 ps) is the Kittel mode, described by the Landau-Lifshitz-Gilbert (LLG) equation:

$$\frac{d\vec{M}}{dt} = -\gamma\mu_0(\vec{M} \times \vec{H}_{\text{eff}}) + \frac{\alpha}{M}\left(\vec{M} \times \frac{d\vec{M}}{dt}\right) \tag{9}$$

- **Why Precession at $B = 0$?** Thin films have strong shape anisotropy (K_u). Laser heating modulates K_u faster than $\vec{M}$ can relax. This sudden change in the "internal field" $\vec{H}_{\text{eff}}$ exerts a torque, launching precession.
- **Unification:** The damping α is physically linked to the ultrafast demagnetization time τ_M: $\tau_M \approx \frac{\hbar}{4k_B T_C \alpha} \approx \frac{1}{R}$ [Koopmans, PRL 2005].

Disentangling Artifacts:

- **Helicity:** Signals $\propto [S(\sigma_+) + S(\sigma_-)]$
- **Linear Dichroism:** Separated by field symmetry. Magnetic signal $\propto [S(+B) - S(-B)]$; Thermal/Acoustic $\propto [S(+B) + S(-B)]$.

Implication: For Nickel ($T_C \approx 631$ K, $\alpha \approx 0.038$), this predicts $\tau_M \approx 100$ fs, matching experimental observations. This confirms that R is a material constant linked to α, independent of laser fluence N.

Helicity Dependent: Circular Polarized Pump (4mW) and Linear Probe

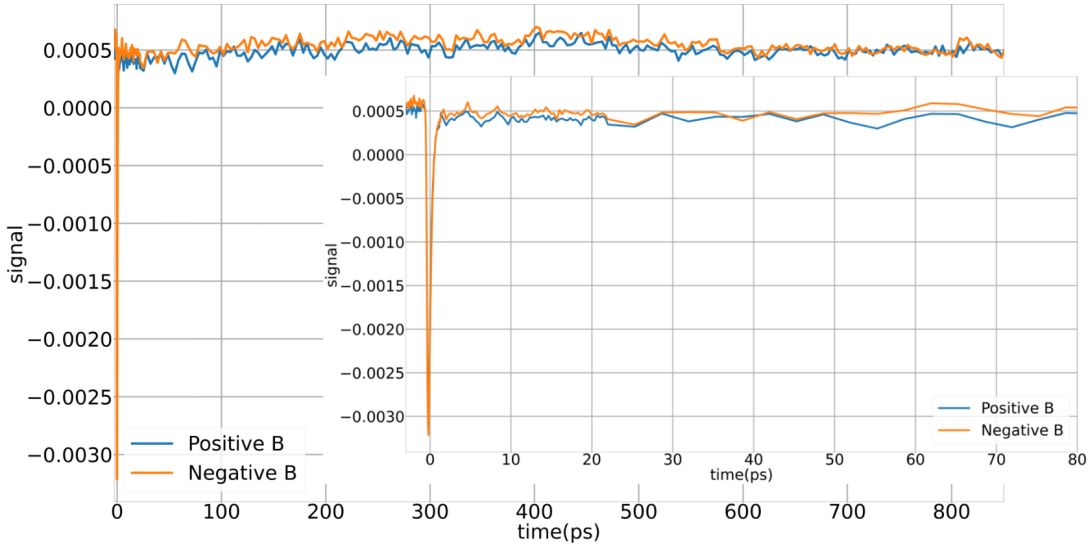

Signal Comparison: 6mW vs 4mW Pump

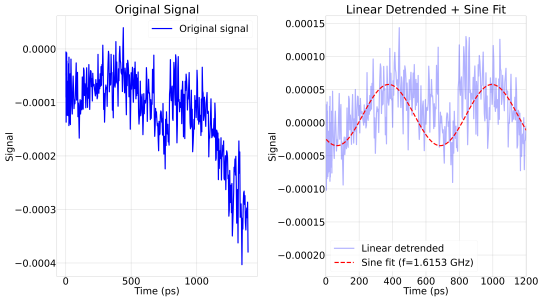

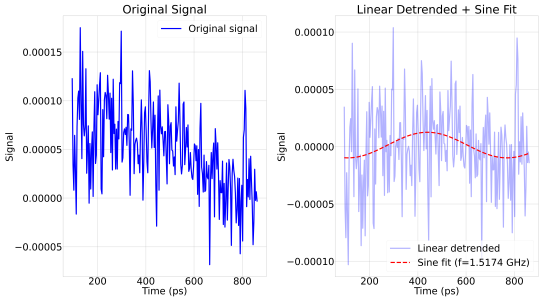

6mW Pump ($1.296 mJ/cm^2$)

Amplitude:
$(4.623 \pm 0.028) \times 10^{-5}$

Frequency:
$(1.615 \pm 0.026) \times 10^{-3}$ THz

Peak ratio: 7.1% of zero delay

4mW Pump ($0.86 mJ/cm^2$)

Amplitude:
$(1.116 \pm 0.322) \times 10^{-5}$

Frequency:
$(1.517 \pm 0.301) \times 10^{-3}$ THz

Peak ratio: 0.4% of zero delay

Specular Inverse Faraday Effect (Dalla Longa et. al., PRB, 2007) + MCD

Linear Pump (6mW) Linear Probe Bifringence: different B's (Zero Corrected)

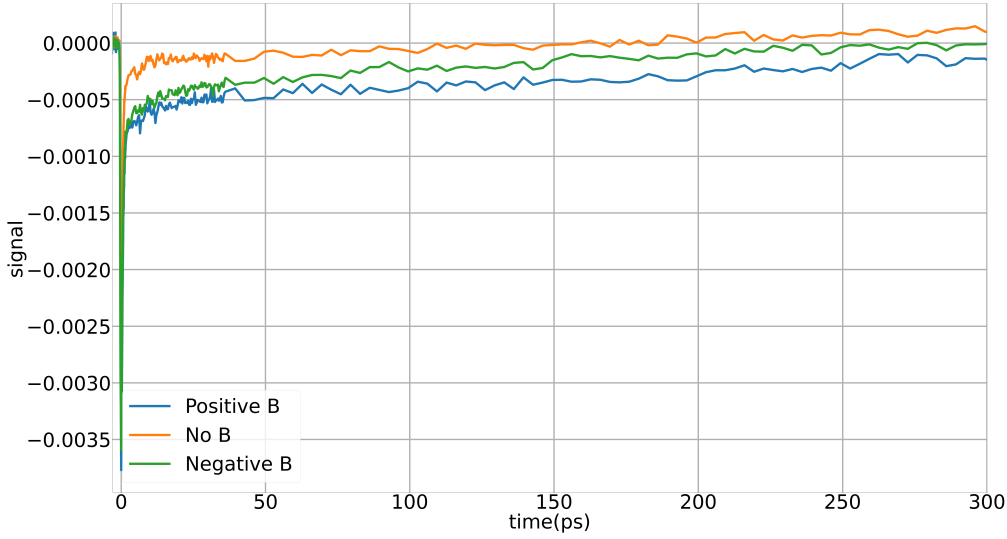

Fitting with Sinusoidal (6mW Bifringence)

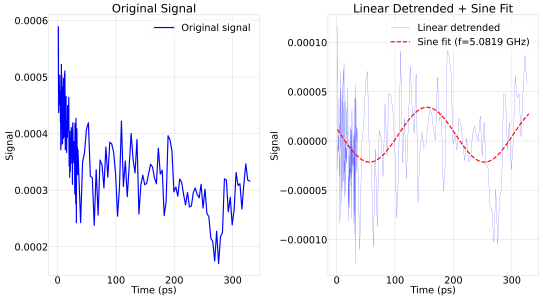

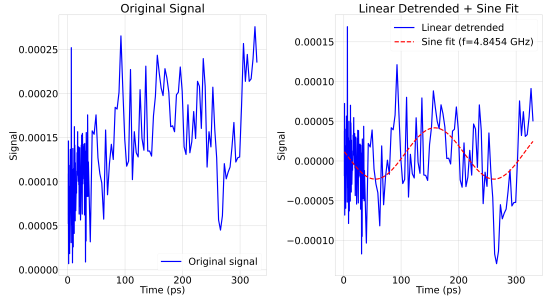

Positive vs No B

Amplitude:
$(2.781 \pm 0.583) \times 10^{-5}$

Frequency:
$(5.082 \pm 0.260) \times 10^{-3}$ THz

Peak ratio: 0.7% of zero delay

Positive vs Negative B

Amplitude:
$(4.542 \pm 0.583) \times 10^{-5}$

Frequency:
$(4.845 \pm 0.160) \times 10^{-3}$ THz

Peak ratio: 1.3% of zero delay

Section 5

Appendix

A.1: The First 100 Femtoseconds: Excitation Physics

What happens when the pulse hits Nickel?

1. **Photon Absorption:** Electrons absorb photons (1.55 eV), creating a highly non-thermal distribution (n_{non-th}) of "hot" carriers above E_F.
2. **e-e Scattering (Thermalization):** Within $\sim 10 - 50$ fs, electron-electron Coulomb scattering redistributes energy, establishing a defined electron temperature $T_e \gg T_l$ (Lattice Temp).
3. **Probing Mechanism:** We measure Transient Reflectivity ($\Delta R/R$).

The Rosei Model (Dielectric Function)

For probe frequencies below the interband transition ($\hbar\omega < E_{interband}$), the change in the real part of the dielectric constant is proportional to the total excess energy of the electron gas:

$$\Delta\epsilon' \propto \Delta U_e \propto \gamma T_e^2 \tag{10}$$

Thus, $\Delta R/R$ maps the cooling of the electron bath.

Citation: Groeneveld, R. H. M., Sprik, R., & Lagendijk, A. *Phys. Rev. B* **51**, 11433 (1995).

A.2: Thermodynamics to Optics: Defining the Energy Reservoirs

1. **Heat Capacities (C_e & C_l)**
   - **Electrons (C_e):** In a metal like Nickel, the electronic specific heat is linear with temperature due to the high density of states at the Fermi level.

$$C_e(T_e) = \gamma T_e$$

     - $\gamma_{Ni} \approx 1065\,\mathrm{J \cdot m^{-3} \cdot K^{-2}}$ (Literature Value for Ni)
   - **Lattice (C_l):** Assumed constant (Debye limit) for $T > \Theta_D$.

$$C_l \approx 3Nk_B \approx \text{Constant}$$

2. **The Rosei Model (Optical Probe Response)**
   - For probe energies below the main interband threshold ($\hbar\omega < E_{ib}$), the change in dielectric function ($\Delta\epsilon$) tracks the **Total Excess Energy** (ΔU) of the system.
   - **Excess Electronic Energy (ΔU_e):**

$$\Delta U_e(t) = \int_{T_0}^{T_e(t)} C_e(T)dT = \frac{1}{2}\gamma(T_e(t)^2 - T_0^2)$$

   - **Excess Lattice Energy (ΔU_l):**

$$\Delta U_l(t) = C_l(T_l(t) - T_0)$$

A.3: The Fitting Model: 2TM Differential Equations

Step 1: Coupled Differential Equations (Physics) We solve for the temperature evolution of the electron (T_e) and lattice (T_l) baths:

$$C_e(T_e)\frac{dT_e}{dt} = -G_{el}(T_e - T_l) + P(t)$$
$$C_l\frac{dT_l}{dt} = +G_{el}(T_e - T_l)$$

- G_{el}: Electron-Phonon Coupling Constant (Fitting Parameter).
- $P(t)$: Laser Source Term (Gaussian pulse, width $\sigma \approx 60$ fs).

Step 2: The Scaling Equation (Optics) To fit the experimental reflectivity data ($\frac{\Delta R}{R}$), we map the calculated temperatures to the optical signal using linear scaling coefficients A and B:

$$\left(\frac{\Delta R}{R}\right)_{fit}(t) = \underbrace{A \cdot [T_e(t)^2 - T_0^2]}_{\text{Electronic (Drude/Rosei)}} + \underbrace{B \cdot [T_l(t) - T_0]}_{\text{Lattice (Strain/Expansion)}}$$

- **A & B:** Scaling factors accounting for the probe sensitivity to electron and lattice energy, respectively.
- This equation links the thermodynamic simulation to the optical measurement.

A.4: Failure of TTM at Low Temperatures

Groeneveld et al. demonstrated that the standard TTM fails to predict relaxation times (τ_E) at low lattice temperatures ($T_l < 50$ K).

The Discrepancy:

- TTM Prediction: In perturbative regimes, $\tau_E \propto T_i$ (Linearly dependent).
- Observation: τ_E saturates and is slower than predicted at low T.

Physical Reason: At low temperatures and low excitation densities, the phase space for electron-electron scattering is restricted by the Pauli exclusion principle. The electron gas **does not** reach a thermal Fermi-Dirac distribution within the pulse duration. This "Non-thermal Electron Model" (NEM) reduces the effective energy transfer rate to the lattice.

Citation: Groeneveld, R. H. M., Sprik, R., & Lagendijk, A. *Phys. Rev. B* **51**, 11433 (1995).

A.5: Phenomenological 3TM (Beaurepaire)

To account for magnetization dynamics, Beaurepaire extended the 2TM to include a spin reservoir (s).
The Three Coupled Equations:

$$C_e \frac{dT_e}{dt} = -G_{el}(T_e - T_l) - G_{es}(T_e - T_s) + P(t) \tag{11}$$

$$C_s \frac{dT_s}{dt} = -G_{es}(T_s - T_e) - G_{sl}(T_s - T_l) \tag{12}$$

$$C_l \frac{dT_l}{dt} = -G_{el}(T_l - T_e) - G_{sl}(T_l - T_s) \tag{13}$$

limitation: This model is purely phenomenological. It treats "spin temperature" as a thermodynamic quantity without explaining *how* angular momentum is dissipated.

Citation: Beaurepaire, E., et al. *Phys. Rev. Lett.* **76**, 4250 (1996).

A.6: Microscopic Three Temperature Model (M3TM)

Koopmans et al. refined the 3TM to address the "Angular Momentum Bottleneck."

Core Concept:

- Demagnetization is driven by **Elliott-Yafet (EY) spin-flip scattering**.
- Probability a_{sf}: The chance an electron flips spin upon scattering with a phonon/impurity.
- R: The material-specific demagnetization rate.

Predicting Spin Temp (T_s)

Since $\Delta R/R$ is non-magnetic, we simulate $m(t)$ via M3TM and **invert** the mean-field equation to find the effective T_s:

Inverse Weiss Mean Field

$$m(t) = \tanh\left(\frac{m(t)\,T_C}{T_s(t)}\right) \tag{14}$$

$$\Rightarrow T_s(t) = \frac{m(t)\cdot T_C}{\operatorname{arctanh}(m(t))} \tag{15}$$

4. Finite-Size Suppression of T_C (Curie Scaling Law):

$$T_C(d) \approx T_C^{\text{bulk}}\left[1 - \left(\frac{d_0}{d}\right)^{\lambda}\right] \approx 500\text{–}550\ \text{K} \tag{16}$$

Citation: Koopmans, B., et al. *Nature Materials* **9**, 259–265 (2010).

A.7: M3TM - Coupling m to Temperatures

Instead of a generic heat equation for spins, M3TM derives the magnetization dynamics $m(t) = M(t)/M_s(0)$ based on the detailed balance of spin-flip rates.

The M3TM Master Equation:

$$\frac{dm}{dt} = Rm\frac{T_l}{T_C}\left(1 - m\coth\left(\frac{mT_C}{T_e}\right)\right) \tag{17}$$

- **Driving Force:** The difference between the electron temperature T_e (disorder source) and the current magnetization state.
- **Dissipation Sink:** The lattice temperature T_l facilitates the angular momentum transfer.

Citation: Koopmans, B., et al. *Nature Materials* **9**, 259–265 (2010).

A.8: Defining the Rate Constant R

The prefactor R in the M3TM equation connects microscopic physics to macroscopic rates.

$$R \propto \frac{a_{sf}\, T_C^2}{\mu_{at}} \tag{18}$$

- a_{sf}: Spin-flip probability (linked to Spin-Orbit Coupling). For Ni, $a_{sf} \approx 0.08 - 0.1$.
- T_C: Curie Temperature.
- μ_{at}: Atomic magnetic moment.

Key Insight: This explains why Ni (high T_C, low μ_{at}) demagnetizes in femtoseconds, while Gd (low T_C, high moment) takes picoseconds. Ni is a "Type I" ultrafast material.

Citation: Koopmans, B., et al. *Nature Materials* **9**, 259–265 (2010).

A.9: Critical Behavior: Diverging Heat Capacity

Using TR-ARPES (Angle-Resolved Photoemission Spectroscopy) and EUV probes, Tengdin et al. observed critical behavior in the electron gas.
Observation: As the pump fluence increases and T_e approaches T_C, the rise in electron temperature saturates.
Implication: There is a divergence in the specific heat of the magnetic system (C_m) near T_C.

$$\int_{T_{init}}^{T_{max}} (C_e(T) + C_m(T))dT = \text{Absorbed Fluence} \tag{19}$$

Energy is rapidly dumped into magnetic fluctuations (spin disorder) rather than increasing kinetic temperature.

Citation: Tengdin, P., et al. *Science Advances* **4**, eaap9744 (2018).

A.10: The "20 fs" Effect

Tengdin's work uncovered a timescale separation previously obscured.

The Discovery

The spin system absorbs sufficient energy to overcome the phase transition barrier ($T_e > T_C$) within the first **20 femtoseconds**.

- The energy transfer to the spin system is extremely fast (likely via superdiffusive transport or exchange interaction).
- However, the *macroscopic* magnetization drop (measured by MOKE) takes ~ 176 fs.
- This implies the system enters a "transient non-equilibrium phase" where the energy condition for demagnetization is met long before the magnetic moment actually vanishes.

Citation: Tengdin, P., et al. *Science Advances* **4**, eaap9744 (2018).

A.11: Crossing T_C for T_e

What does it mean for T_e to cross T_C while the lattice (T_l) is still cold?

- **Fluence Independence:** Once $T_e > T_C$, the demagnetization time ($\tau_M \approx 176$ fs) becomes independent of fluence. The bottleneck is no longer energy availability, but the microscopic relaxation rate (magnon generation).
- **Recovery Bifurcation:**
  - If $T_e < T_C$: Fast recovery (~ 500 fs).
  - If $T_e > T_C$: Slow recovery (~ 76 ps) because the system must recover from a complete paramagnetic-like disorder.

Citation: Tengdin, P., et al. *Science Advances* **4**, eaap9744 (2018).

A.12: Setup for Helicity Dependent Studies

To test if photons directly transfer angular momentum to spins, we use Anisotropic Pump-Probe.
Configuration:

- **Pump:** Circularly Polarized (σ^+ or σ^-) or Linear.
- **Probe:** Linearly Polarized.
- **Detection:** A Quarter Wave Plate (QWP) is placed *before* the balanced detector.

Purpose of QWP in Detection: It allows the measurement of *Ellipticity* changes in the probe beam, which helps distinguish between true Magnetic Kerr effects and optical artifacts (like SIFE).

Citation: Dalla Longa, F., et al. *Phys. Rev. B* **75**, 224431 (2007).

A.13: Does Photon Helicity Drive Demag?

Hypothesis: If photons transfer angular momentum $\pm\hbar$ directly to spins (Inverse Faraday Effect - IFE), then:

- σ^+ pump should demagnetize differently than σ^- pump (depending on sample magnetization M).
- Specifically, parallel alignment should hinder demag, anti-parallel should enhance it.

Result: In Ni, Dalla Longa et al. showed that demagnetization amplitude and time τ_M are **independent** of pump helicity.

Citation: Dalla Longa, F., et al. *Phys. Rev. B* **75**, 224431 (2007).

A.14: Disentangling Artifacts

When pumping with circular light, we see differences in the signal. We must distinguish:

1. **MCD (Magnetic Circular Dichroism):** Differential *absorption* of σ^+ vs σ^-. One helicity deposits more energy, leading to higher T_e, and thus more thermal demagnetization. This is a thermal effect.
2. **IFE (Inverse Faraday Effect):** Coherent generation of a magnetic field by the light pulse. This is a non-thermal, opto-magnetic effect.

In Ni, the observed helicity dependence is dominated by MCD (thermal bleaching), not coherent switching.

Citation: Koopmans, B., et al. *Nat. Mater.* (2010); Dalla Longa et al. (2007).

A.15: Linear Pump - Linear Probe Physics

Effect of Linear Pump:

- Deposits energy ($P(t)$) without net angular momentum transfer.
- Creates the hot electron bath driving the M3TM equations.

QWP Detection (Birefringence): By rotating the QWP before the detector, we can separate the *rotation* (Kerr rotation $\theta_K \propto M$) from the *ellipticity* changes induced by transient changes in the dielectric tensor (non-magnetic artifacts). This ensures we are measuring real magnetization dynamics, not just optical bleaching.

Citation: Wilks, R., et al. *J. Appl. Phys.* **95**, 7441 (2004).

A.16: M3TM - The Equilibration Regime

The Analytical Solution (Approximated):
For type I materials (Ni), where $\tau_M \ll \tau_{ep}$ (electron-phonon relaxation):

$$\tau_M \approx \frac{\mu_{at}}{4\alpha_G k_B T_C} \tag{20}$$

Where α_G is the Gilbert damping parameter.
This connects the ultrafast (femtosecond) demagnetization directly to the nanosecond precession damping parameter α, providing a unified picture of spin dynamics across timescales.

Citation: Koopmans, B., et al. *Phys. Rev. Lett.* **95**, 267207 (2005).

A.17: Transport Effects in Thin Films

Although we focus on local dynamics, Groeneveld's work on Au/Ag highlights that in thin films (30-45nm), ballistic and diffusive transport matters.

- **Ballistic Time:** $\tau_{bal} \approx d/v_F \approx 20 - 30$ fs.
- **Diffusive Time:** $\tau_{diff} \approx C_e d^2/2\kappa$.

For our Ni film ($\sim$ 10nm), transport is faster than the pulse duration. We can assume homogeneous heating in the depth (z) direction, validating the use of localized M3TM/2TM equations without spatial gradient terms.

Citation: Groeneveld, R. H. M., et al. *PRB* 51 (1995).

A.18: Resolving the Timescale Discrepancy

Paradox: Why does the phase transition energy transfer happen in < 20 fs, but MOKE shows ~ 176 fs decay?
Resolution:

1. **Energy vs. Order:** The energy required to destroy magnetic order is absorbed by the spin system immediately (creating high-energy magnons/stochastic spin disorder).
2. **Observable Lag:** The MOKE signal (probing k-space averaged band structure) reflects the macroscopic loss of moment, which requires the decoherence of the spin ensemble.

The "demagnetization time" is the time taken for the system to *express* the disorder that was energetically mandated in the first 20 fs.

Citation: Tengdin, P., et al. *Science Advances* **4** (2018).

A.19: Key Parameters for Nickel Simulation

To reproduce these results in 2TM/M3TM, the following parameters are critical:

- **Curie Temp (T_C):** 631 K (500K after adjustment).
- **Magnetic Moment (μ_{at}):** $0.62\mu_B$.
- **Spin-flip probability (a_{sf}):** $\approx 0.08 - 0.2$ (High compared to other metals).
- **e-ph Coupling (g_∞):** $\approx 3 \times 10^{17}$ $\mathrm{Wm^{-3}K^{-1}}$.(9 after calculating)
- **e-e Scattering Rate (K):** 0.10 ± 0.05 $\mathrm{fs^{-1}eV^{-2}}$.(litrature)

These values dictate the "Type I" fast demagnetization behavior.

Data compiled from Koopmans (2010) and Groeneveld (1995).